Can Ningaloo Niño/Niña develop without El Niño-Southern oscillation?

Takahito Kataoka, Sébastien Masson, Takeshi Izumo, Tomoki Tozuka, Toshio Yamagata

AGU100 ADVANCING EARTH AND SPACE SCIENCE

Geophysical Research Letters

RESEARCH LETTER
10.1029/2018GL078188

Special Section:
Midlatitude Marine Heatwaves: Forcing and Impacts

Can Ningaloo Niño/Niña Develop Without El Niño–Southern Oscillation?

Takahito Kataoka[1], Sébastien Masson[2], Takeshi Izumo[2], Tomoki Tozuka[3,4], and Toshio Yamagata[4]

[1]Project Team for Advanced Climate Modeling, JAMSTEC, Yokohama, Japan, [2]LOCEAN/IPSL, Université Pierre et Marie Curie, Paris, France, [3]Department of Earth and Planetary Science, Graduate School of Science, The University of Tokyo, Tokyo, Japan, [4]Application Laboratory, JAMSTEC, Yokohama, Japan

Key Points:
- Ningaloo Niño/Niña can occur even without ENSO
- Its amplitude, duration, and seasonality in a *no-ENSO world* are comparable to those in the observations and the model control run
- Local air-sea coupled feedback contributes to the development without ENSO, amplifying atmospheric stochastic forcing

Supporting Information:
- Supporting Information S1

Correspondence to:
T. Kataoka,
tkataoka@15.alumni.u-tokyo.ac.jp

Citation:
Kataoka, T., Masson, S., Izumo, T., Tozuka, T., & Yamagata, T. (2018). Can Ningaloo Niño/Niña develop without El Niño–Southern Oscillation? *Geophysical Research Letters*, *45*, 7040–7048. https://doi.org/10.1029/2018GL078188

Received 3 APR 2018
Accepted 22 JUN 2018
Accepted article online 5 JUL 2018
Published online 16 JUL 2018

Abstract Ningaloo Niño/Niña is the dominant climate mode in the southeastern Indian Ocean with its center of positive/negative sea surface temperature anomalies attached to Australia. Ningaloo Niño is the major cause of marine heatwaves in the region. Although oceanic variability in this region has long been considered mainly as a response to the El Niño–Southern Oscillation (ENSO), some recent studies have suggested the possible existence of local air-sea feedback processes. Using a state-of-the-art ocean-atmosphere coupled model that realistically simulates Ningaloo Niño/Niña, whether Ningaloo Niño/Niña can occur independently of ENSO is examined. Even in an experiment in which ENSO is suppressed by strongly nudging tropical Pacific sea surface temperatures toward the model climatology, Ningaloo Niño/Niña with a similar magnitude and seasonality still develops, likely through an air-sea interaction off Western Australia amplifying atmospheric stochastic forcing. This study is the first to show that Ningaloo Niño/Niña can develop even without ENSO.

Plain Language Summary Ningaloo Niño/Niña is the major cause of extreme warming/cooling in the southeastern Indian Ocean in austral summer and affects the marine environment and precipitation over the Western Australia. Although it has long been considered that El Niño and La Niña in the Pacific drive ocean extreme events in this region, some recent studies have suggested a possibility that warming/cooling off Western Australia would add to itself by changing the atmospheric condition and creating further heating/cooling (i.e., positive air-sea feedback). Using climate model simulations, we show that, even without El Niño and La Niña, Ningaloo Niño/Niña with a similar magnitude occurs in summer, likely through the positive air-sea feedback off Western Australia amplifying atmospheric random forcing. This study is the first to show that Ningaloo Niño/Niña can develop even without El Niño and La Niña.

1. Introduction

Ningaloo Niño/Niña is the dominant mode of climate variability off the west coast of Australia (M. Feng, McPhaden, et al., 2013; Kataoka et al., 2014). This phenomenon is associated with positive/negative sea surface temperature (SST) anomalies off Western Australia and typically develops during austral spring and peaks in austral summer (Kataoka et al., 2014). Observations and proxy data suggest that Ningaloo Niño occurs every 3–5 years on average (M. Feng et al., 2015; Kataoka et al., 2014; Zinke et al., 2014). Among others, an unprecedented marine heatwave event hit the west coast of Australia in the austral summer of 2010/2011, resulting in devastating coral bleaching (Depczynski et al., 2013; Pearce & Feng, 2013) and changes in biodiversity patterns (Wernberg et al., 2013). As well as affecting the marine environment, Ningaloo Niño also induces precipitation anomalies over Western Australia (Tozuka et al., 2014), a region much affected by rainfall variability (e.g., Turner & Asseng, 2005). The driving mechanisms of Australian marine heatwaves, however, are little known (Perkins-Kirkpatrick et al., 2016). Hence, understanding Ningaloo Niño is of great importance.

Interannual oceanic variability off the western coast of Australia has long been considered to be mainly a response to tropical Pacific variability, especially the El Niño–Southern Oscillation (ENSO; M. Feng et al., 2008; M. Feng, McPhaden, et al., 2013; Pariwano et al., 1986; Wijffels & Meyers, 2003). However, Kataoka et al. (2014) showed that some Ningaloo Niño events develop through an intrinsic air-sea interaction off the west coast of Australia: an anomalous low generated by positive SST anomalies (Tozuka et al., 2014)

forces northerly alongshore wind anomalies due to the land-sea pressure contrast, which in turn cause coastal downwelling anomalies and further enhance the initial warm SST anomalies through a strengthened poleward-flowing Leeuwin Current (Benthuysen et al., 2014; Kataoka et al., 2017; Marshall et al., 2015). A subsequent study by Marshall et al. (2015) also concluded that Ningaloo Niño is the result of a combination of a local ocean-atmosphere coupled process and remote forcing. While both Kataoka et al. (2014) and Marshall et al. (2015) suggested that latent heat flux anomalies contribute to the growth of offshore SST anomalies, a recent study using an ocean general circulation model underlined the importance of the enhanced warming by the climatological shortwave radiation due to the shallower mixed-layer depth (MLD) associated with reduced wind speed, offering another possible feedback (Kataoka et al., 2017; see also Morioka et al., 2010, for the importance of the MLD anomaly in generating SST anomalies in the southern Indian Ocean).

Then, a simple question arises. Would Ningaloo Niño exist even without ENSO? Considering that Ningaloo Niño in 1982/1983 and 2010/2011 occurred during very strong El Niño and La Niña events, respectively (Kataoka et al., 2014; Marshall et al., 2015), the answer seems to be yes. The fuzzy relationship between Ningaloo Niño and ENSO is also reflected in a relatively low correlation coefficient of −0.4 at most on the interannual time scale (supporting information Figure S1). However, as long as ENSO exists (it does in the real world), ENSO influence including its delayed effects (e.g., Xie et al., 2009), which is nonlinear, cannot be completely removed from the observational data. Therefore, neither the co-occurrence with El Niño and La Niña nor the low correlation coefficient with an ENSO index provides a definitive answer to the above question.

In this study, using a state-of-the-art coupled general circulation model (CGCM), we demonstrate that Ningaloo Niño exists even when the tropical Pacific interannual variability is suppressed. While Ningaloo Niño and Niña show some asymmetry (e.g., Tozuka et al., 2014), the previous studies suggested that they may be considered as a mirror image to the first order (Kataoka et al., 2014, 2017; Tozuka et al., 2014), which motivates us to adopt linear analyses here.

2. Model and Data Description

The CGCM used in this study is SINTEX-F2 (Masson et al., 2012). The atmospheric component is ECHAM 5.3 (Roeckner et al., 2003, 2004), and its horizontal resolution is T106 with 31 hybrid sigma-pressure levels in the vertical. A cumulus convection scheme developed by Tiedtke (1989) and Nordeng (1994) is used. The oceanic component is NEMO (Madec, 2008) with the ORCA05 horizontal grid (resolution ~0.5°) and 31 vertical levels. LIM2 ice model (Timmermann et al., 2005) is also included with the OASIS3 coupler (Valcke, 2006). Successful studies on Indo-Pacific climate using SINTEX-F2 (Doi et al., 2016; Masson et al., 2012; Prodhomme et al., 2015; Sasaki et al., 2015; Terray et al., 2012) give us confidence to use this model for studying a phenomenon affected by ENSO.

Two experiments are conducted in the present study. In the control (CTRL) run, the ocean and atmosphere are freely coupled everywhere. On the other hand, in the noENSO run, the ocean and atmosphere are allowed to interact everywhere except over the tropical Pacific and the maritime continent (supporting information Figure S2), where SSTs are strongly restored to the smooth daily climatology of the CTRL run. Both experiments are integrated for 110 years. A spin-up period of the first 10 years is discarded (the CTRL experiment was actually run for 210 years, for statistical sensitivity tests; not shown). The configuration of the noENSO run is identical to the FTPC run of Prodhomme et al. (2015), except that the noENSO experiment has a longer duration.

For comparison with the observations, we use (1) the Extended Reconstructed SST (ERSST) version3b data set (Smith et al., 2008) from 1950 to 2017, (2) the National Centers for Environmental Prediction/National Center for Atmospheric Research reanalysis data (Kalnay et al., 1996) for sea level pressure (SLP), wind at 10 m, and precipitation for 1950–2017, (3) the Global Precipitation Climatology Project (Adler et al., 2003) precipitation from 1979 to 2017, (4) the sea surface height (SSH), and ocean currents derived from the Simple Ocean Data Assimilation (Carton & Giese, 2008) version 2.2.4 from 1950 to 2010, and (5) the National Oceanic and Atmospheric Administration interpolated outgoing longwave radiation (Liebmann & Smith, 1996) for 1975–2016.

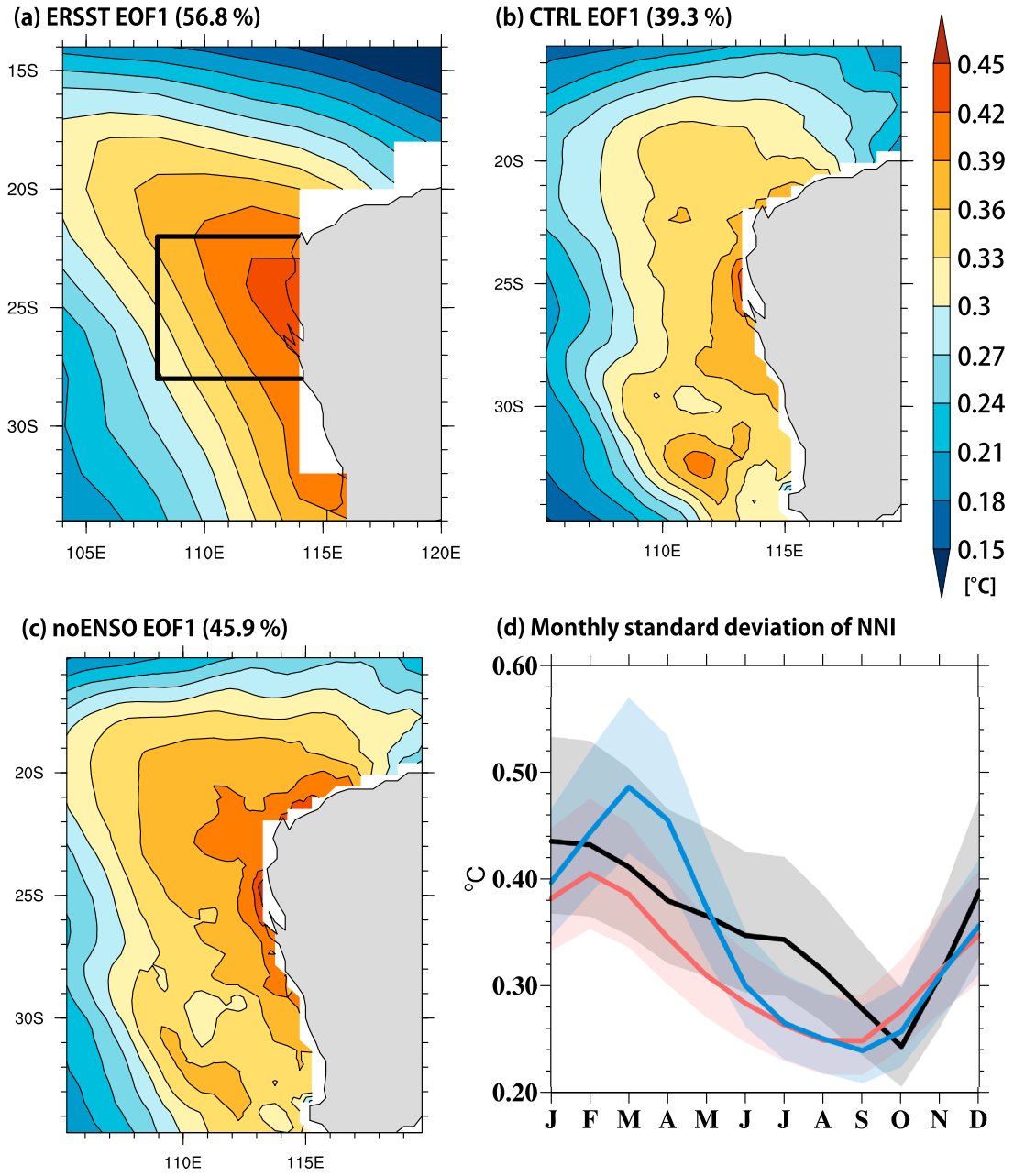

Figure 1. First empirical orthogonal function (EOF) mode of sea surface temperature (SST) anomalies off Western Australia for (a) Extended Reconstructed SST (ERSST), (b) control (CTRL) run, and (c) noENSO run. The slight difference in the domain for ERSST is due to its coarse resolution. The variance explained by the first EOF is indicated in brackets. In panel (a), the domain used to calculate the Ningaloo Niño index (NNI; 108°E—coast, 28–22°S) is superimposed (black line). (d) Monthly standard deviation of the 3-month running averaged NNI (black: ERSST, red: control [CTRL] run, and blue: noENSO run). Shading represents the 95% confidence interval from a two-tailed chi-square test.

Trends are removed from all of the time series using a linear least squares fit. Then, to remove decadal variability (Kuhnert et al., 1999; Zinke et al., 2014), a Lanczos high-pass filter (Duchon, 1979) is applied except for the shorter Global Precipitation Climatology Project data set, with the first and last 5 years of each time series discarded to avoid edge effects. The response curve of this filter retains 50% of the amplitude at 8-year period and ~90% at 5-year period. Qualitatively, the same results are obtained even when a filter that has a sharper rolloff (50% amplitude at 8-year period and 90% at 6-year period) with the first and last 10 years discarded.

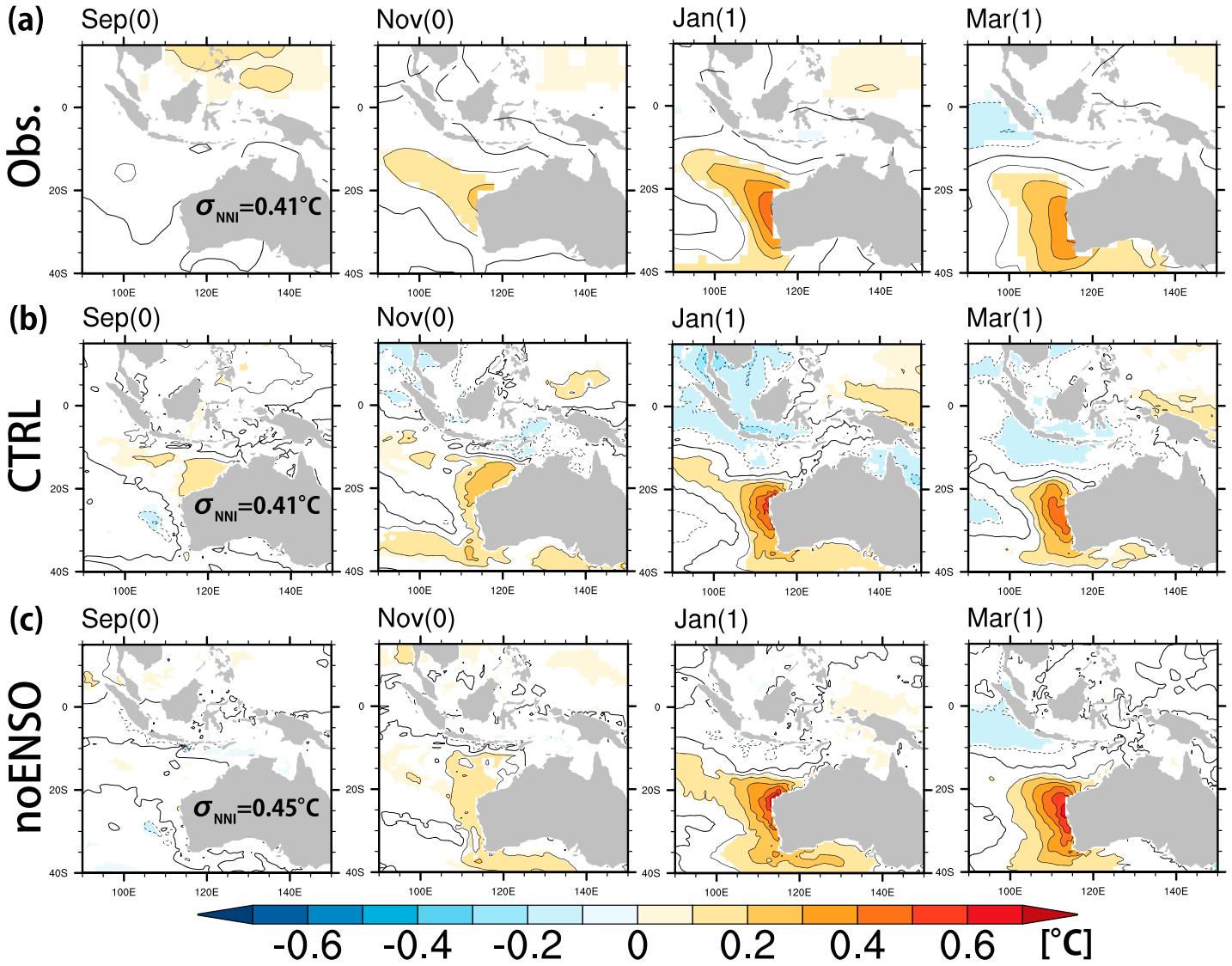

Figure 2. Regressed anomalies of sea surface temperature (in °C) onto the normalized JFM-mean Ningaloo Niño index (NNI) for (a) the observation, (b) control (CTRL), and (c) noENSO. Results are shown every 2 months from September (0) to March (1). Contour intervals are 0.1 °C. Regression coefficients exceeding the 95% confidence level by a two-tailed *t* test are shaded. The standard deviations used for the normalization are indicated on the panels for Sep (0).

3. Results

3.1. CTRL Run

To extract the dominant mode of variability off the western coast of Australia (105–120°E, 35–15°S; Figures 1a and 1b), we perform an empirical orthogonal function analysis of monthly SST anomalies. The CTRL run reproduces Ningaloo Niño well with a similar spatial pattern and amplitude to the observations. The pattern correlation on the observation grid is 0.78, which is among the best in the state-of-the-art coupled models (Kido et al., 2016). Following Kataoka et al. (2014), the Ningaloo Niño index (NNI) is defined by area-averaged SST anomalies off the west coast of Australia (108°E—the coast and 22–28°S). To check the model performance in Ningaloo Niño seasonality, the standard deviation of the NNI is computed as a function of the calendar month (Figure 1d). The model captures the seasonality well with a peak from January to March (JFM), though the variability is slightly lower than that in the observation in austral winter. Hereafter, year 0 (1) denotes the Ningaloo Niño-developing year (the following year).

To see the spatiotemporal evolution of Ningaloo Niño in the model, a lead-lag regression analysis of SST anomalies onto the normalized JFM-mean NNI is performed on the model outputs along with the

observations (Figures 2a and 2b). The model captures the SST evolution well: SST anomalies appear to the northwest of Australia in austral spring and peak around summer, adjacent to North West Cape.

Regarding the generation mechanism, SINTEX-F2 again reproduces observed features reasonably well. Positive SSH anomalies, that is, coastal downwelling waves, are seen (Figure 3d), partly originating from the western Pacific (Clarke, 1991; Clarke & Liu, 1994; Meyers, 1996), where observed SSH signals are more modest than in the CTRL run (Figure 3a), and partly forced locally by alongshore wind as suggested by the poleward strengthening of SSH anomalies. These coastal waves intensify the Leeuwin Current (Figures 3a and 3d), which causes warm advection anomalies (Benthuysen et al., 2014; Kataoka et al., 2017; Marshall et al., 2015). Negative SLP and alongshore-northerly wind anomalies off the western coast of Australia are also found (Figures 3b and 3e). The model simulates the atmospheric circulation anomalies relatively well, although the minima in the CTRL run are slightly shifted eastward. These atmospheric anomalies have both western tropical Pacific and local forcing origins (Tozuka et al., 2014).

3.2. noENSO Run

Since the CTRL run well reproduces Ningaloo Niño, we expect that it can provide a useful insight into controversial ENSO-Ningaloo Niño connection. As with the CTRL run, an empirical orthogonal function analysis is conducted on SST anomalies of the noENSO experiment over the same domain (Figure 1c). It is found that Ningaloo Niño is still present and remains the dominant mode even without ENSO. The monthly standard deviation of the NNI for the noENSO run reveals that its seasonal phase-locking nature also remains almost unchanged (Figure 1d). Although the 95% confidence intervals overlap, we see some difference in the amplitude between the CTRL and noENSO experiments; a brief consideration will be given later. The most important point here is that the amplitude of Ningaloo Niño is unlikely smaller without ENSO.

A lead-lag regression analysis of SST anomalies onto the normalized JFM-mean NNI reveals that Ningaloo Niño in the noENSO experiment is not just a transient signal but that it evolves with time as in the real world and the CTRL run (Figure 2c; see also supporting information Figure S3). The same regression analysis but for other anomaly fields is also performed to look into the generation mechanism of Ningaloo Niño independent from ENSO. As expected, almost no significant coastal waves from the western Pacific are found in this experiment (Figure 3g), but positive SSH anomalies are seen along the coast, suggesting a local oceanic dynamical response to local alongshore wind anomalies off Western Australia (Figure 3h).

As in the observations and the CTRL run, negative SLP anomalies are found off the western coast of Australia around the peak phase of Ningaloo Niño in the noENSO run (Figure 3h). It is important to note that neither significant SST anomalies associated with a particular climate mode (e.g., the Indian Ocean Dipole; Saji et al., 1999) nor an atmospheric teleconnection that may contribute to the generation of atmospheric circulation anomalies related to Ningaloo Niño are found (supporting information Figures S4b and S4e). Therefore, the negative SLP anomalies in the southeastern Indian Ocean can be related to local SST anomalies. Positive SST anomalies generate low SLP anomalies off Western Australia through more active convection to the northwest of Australia and the related Matsuno (1966)-Gill (1980) response to an off-equatorial heating (with SLP shifted westward of the diabatic heating anomaly as it emits Rossby waves), a consistent feature among the observations and the model experiments (Figures 3c, 3f, and 3i and supporting information Figure S5; and in agreement with the local SST-forced atmospheric model experiments of Tozuka et al., 2014). The anomalous low is accompanied by alongshore-northerly wind anomalies, which cause coastal downwelling anomalies as discussed above (Figure 3h). These coastal downwelling anomalies enhance the initial SST anomalies via a stronger poleward-flowing current (Kataoka et al., 2017; Marshall et al., 2015). In addition, the cyclonic wind anomalies are against the climatological anticyclonic wind, which results in reduced wind speeds and thus shallower MLDs (supporting information Figure S6), consistent with the CTRL run and a previous oceanic modeling study (Kataoka et al., 2017). Thus, the local feedback processes seem to operate, at least along and off the northwest coast where climatological SSTs are close enough to the atmospheric deep convection threshold (~28 °C, e.g., Gadgil et al., 1984) so that SST anomalies can influence atmospheric convection/precipitation. The absence of ENSO in austral spring could offer favorable conditions for local SST forcing because La Niña tends to suppress the atmospheric convection off Western Australia (supporting information Figure S7) and thus, may explain the difference in the amplitude of Ningaloo Niño between the CTRL and noENSO experiment. We note that while latent heat loss is reduced over the offshore region (supporting information Figure S6), which also favors shallower MLD, its direct

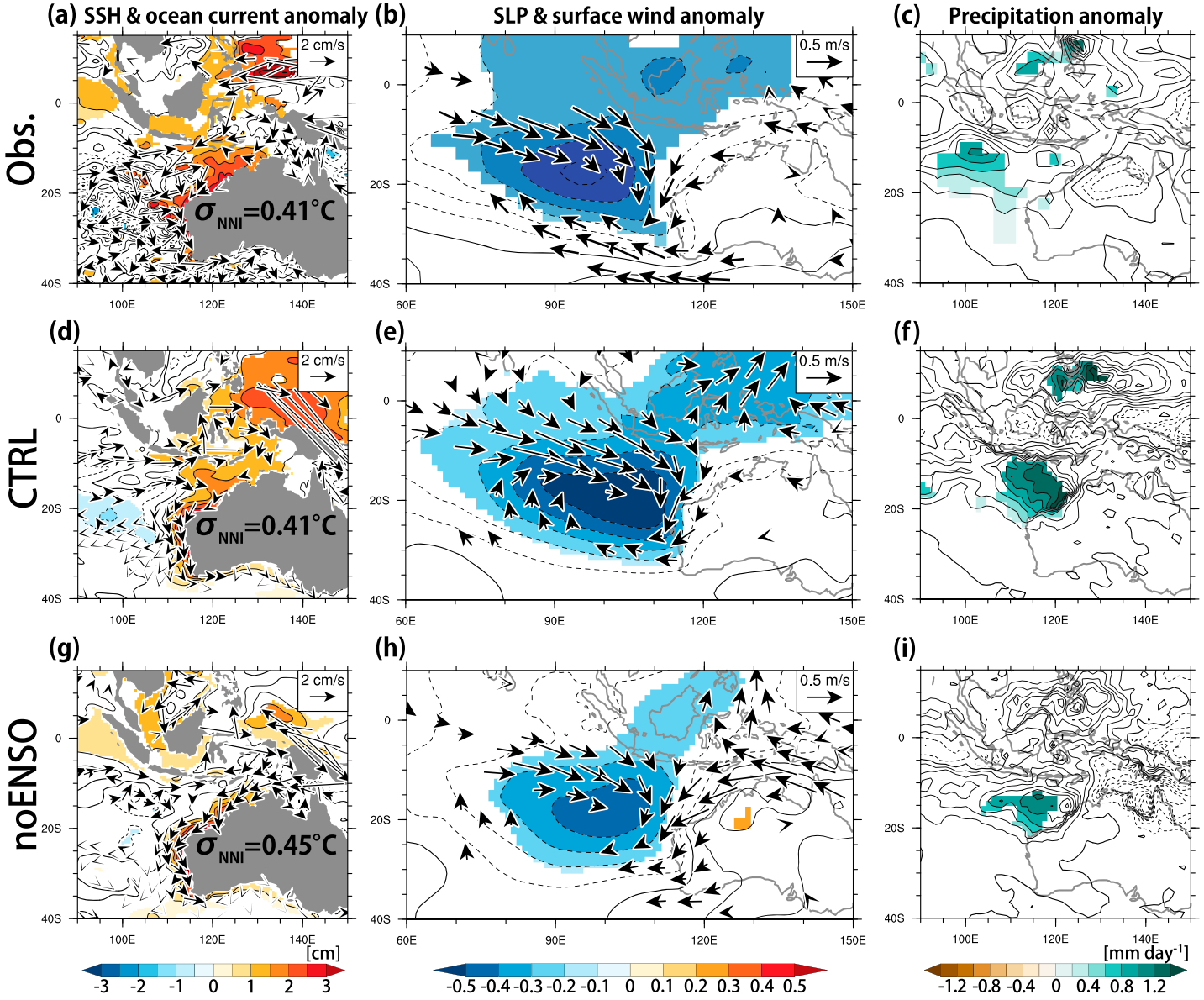

Figure 3. DJF-averaged maps of regression coefficients for (a) sea surface height (SSH; in cm) and the upper 50-m ocean current (in cm/s), (b) standardized sea level pressure and surface wind (in m/s), and (c) precipitation (mm/day) anomalies from the reanalysis and observational data against the JFM-mean Ningaloo Niño index (NNI). Sea level pressure anomalies are normalized by the standard deviations at each grid point. (d–f) As in (a–c) but for control (CTRL). (g–i) As in (a–c) but for noENSO. Coefficients significant at the 95% confidence level according to a two-tailed *t* test are shaded except for the assimilated SSH and observed precipitation anomalies for which the 90% confidence level is adopted. Vectors are drawn when the zonal or meridional component is significant at the 95% level except for ocean current anomalies from Simple Ocean Data Assimilation for which the 90% confidence level is adopted. The standard deviations used for the normalization are shown on the panels for SSH anomaly.

warming effect is offset by the enhanced cooling by the climatological latent heat flux according to Kataoka et al. (2017).

Regarding initial perturbations to be amplified by the regional feedback, the above-mentioned absence of significant anomalies related to a large-scale climate mode such as the Indian Ocean Dipole indicates that atmospheric internal variability may be a candidate; for example, variations in the strength/position of the south Indian Ocean anticyclone, or the Madden-Julian Oscillation (Madden & Julian, 1971, 1972) are known to force SST/precipitation anomalies to the northwest of Australia (e.g., J. Feng, Li, & Xu, 2013; Marshall &

Hendon, 2014; Vialard et al., 2013). Also, such atmospheric stochastic variability could modulate the growth of Ningaloo Niño, but we leave the details of their possible roles for a future study.

4. Conclusions and Discussions

We performed two CGCM experiments and demonstrated that in the *noENSO* sensitivity experiment, Ningaloo Niño/Niña develops even without ENSO with a similar amplitude, duration, and seasonality. The driving mechanism seems to be the intrinsic air-sea interaction off the west coast of Australia shown in earlier studies (e.g., Kataoka et al., 2014, 2017; Tozuka et al., 2014), which can amplify initial atmospheric or oceanic perturbations. In this positive air-sea feedback, a local warm SST anomaly would strengthen atmospheric deep convection to the northwest of Australia, which is accompanied by low SLP anomalies off Western Australia, northwesterlies extending westward of the convection anomaly, and alongshore-northerly wind anomalies (Matsuno-Gill response). These alongshore wind anomalies, in turn, feedback onto initial SST anomalies by causing coastal downwelling anomalies through stronger poleward-flowing current (e.g., Kataoka et al., 2017; Marshall et al., 2015). Furthermore, the northwesterly anomalies northwest of Australia oppose the mean wind and reduce the evaporation, thereby shallowing the MLD. This shallowing contributes to offshore SST anomalies by enhancing the climatological warming by the shortwave radiation (Kataoka et al., 2017). These processes (and *vice versa* for a Ningaloo Niña) favor an amplification, or at least a sustainment, of the initial SST (or atmospheric) anomalies.

The present study is the first to show the existence of Ningaloo Niño/Niña events in a *no-ENSO world*. This does not, however, mean that Ningaloo Niño/Niña is not related to ENSO (correlation coefficient between the NNI and Niño3.4 is close to 0.4; supporting information Figure S1). Remote forcing from the tropical Pacific contributes to its variability via both atmospheric and oceanic bridges (Clarke & Li, 2004; M. Feng et al., 2004; Tozuka et al., 2014; Zhang et al., 2017; Zinke et al., 2014). In addition, M. Feng et al. (2015) showed that the recent negative Interdecadal Pacific Oscillation influenced the warm condition in the southeastern Indian Ocean. The warmer mean state could favor the local air-sea coupling (e.g., Doi et al., 2015) and, thus, for the local positive feedback process.

Since marine heatwaves off North America (Yuan & Yamagata, 2014) and Northern Africa (Oettli et al., 2016) are shown to develop through a similar mechanism to the Ningaloo Niño, the insight obtained here may help to understand such similar coastal Niños. However, the climatological SSTs off Western Australia are unique in that they are higher than those at the same latitudes because of the absence of upwelling and the presence of the poleward-flowing Leeuwin Current (supporting information Figure S8). The background difference may modulate the coupled ocean-atmosphere process in each eastern boundary region as discussed above.

Finally, our results suggest that there are triggering processes related neither to ENSO nor to atmospheric teleconnections from other basins. Atmospheric internal variability may be a candidate, and such atmospheric stochastic variability could modulate the SST variability in the Ningaloo Niño region as well. Quantifying the relative contributions of stochastic atmospheric forcing, the local feedback, and external forcing such as ENSO is a possible topic for future studies.

Acknowledgments

We would like to thank Hiroaki Miura and Tamaki Suematsu for helpful discussions, Takeshi Doi for technical advice, and two anonymous reviewers for helpful comments. Much of this work was conducted when T. K. was at LOCEAN with financial support from MEXT, Japan. The present research was supported by MEXT through the Integrated Research Program for Advancing Climate Models and by the Japan Society for Promotion of Science through Grant-in-Aid for Scientific Research (B) JP16H04047. T. K. was supported by a Research Fellowship of the Japan Society for the Promotion of Science (JSPS) for Young Scientists and MEXT, Japan. The ERSST, NCEP/NCAR reanalysis, GPCP data, and NOAA-interpolated OLR were provided by the NOAA/OAR/ESRL PSD, Boulder, Colorado, USA, from their web site at http://www.esrl.noaa.gov/psd/; SODA at http://apdrc.soest.hawaii.edu/. This work was performed using HPC resources from GENCI-IDRIS (grants 2013-016895 and 2014-016895).

References

Adler, R. F., Huffman, G. J., Chang, A., Ferraro, R., Xie, P., Janowiak, J., et al. (2003). The version 2 Global Precipitation Climatology Project (GPCP) monthly precipitation analysis (1979-present). *Journal of Hydrometeorology*, *4*(6), 1147–1167. https://doi.org/10.1175/1525-7541(2003)004%3C1147:TVGPCP%3E2.0.CO;2

Benthuysen, J., Feng, M., & Zhong, L. (2014). Spatial patterns of warming off Western Australia during the 2011 Ningaloo Niño: Quantifying impacts of remote and local forcing. *Continental Shelf Research*, *91*, 232–246. https://doi.org/10.1016/j.csr.2014.09.014

Carton, J. A., & Giese, S. G. (2008). A reanalysis of ocean climate using Simple Ocean Data Assimilation (SODA). *Monthly Weather Review*, *136*(8), 2999–3017. https://doi.org/10.1175/2007MWR1978.1

Clarke, A. J. (1991). On the reflection and transmission of low-frequency energy at the irregular western Pacific Ocean boundary. *Journal of Geophysical Research*, *96*(S01), 3289–3305. https://doi.org/10.1029/90JC00985

Clarke, A. J., & Li, J. (2004). El Niño/La Niña shelf edge flow and Australian western rock lobsters. *Geophysical Research Letters*, *31*, L11301. https://doi.org/10.1029/2003GL018900

Clarke, A. J., & Liu, X. (1994). Interannual sea level in the northern and eastern Indian Ocean. *Journal of Physical Oceanography*, *24*(6), 1224–1235. https://doi.org/10.1175/1520-0485(1994)024%3C1224:ISLITN%3E2.0.CO;2

Depczynski, M., Gilmour, J. P., Ridgway, T., Barnes, H., Heyward, A. J., Holmes, T. H., et al. (2013). Bleaching, coral mortality and subsequent survivorship on a West Australian fringing reef. *Coral Reefs*, *32*(1), 233–238. https://doi.org/10.1007/s00338-012-0974-0

Doi, T., Behera, S. K., & Yamagata, T. (2015). An interdecadal regime shift in rainfall predictability related to the Ningaloo Niño in the late 1990s. *Journal of Geophysical Research: Oceans*, *120*, 1388–1396. https://doi.org/10.1002/2014JC010562

Doi, T., Behera, S. K., & Yamagata, T. (2016). Improved seasonal prediction using the SINTEX-F2 coupled model. *Journal of Advances in Modeling Earth Systems*, *8*(4), 1847–1867. https://doi.org/10.1002/2016MS000744

Duchon, C. E. (1979). Lanczos filtering in one and two dimensions. *Journal of Applied Meteorology*, *18*(8), 1016–1022. https://doi.org/10.1175/1520-0450(1979)018%3C1016:LFIOAT%3E2.0.CO;2

Feng, J., Li, J., & Xu, H. (2013). Increased summer rainfall in northwest Australia linked to southern Indian Ocean climate variability. *Journal of Geophysical Research: Atmospheres*, *118*, 467–480. https://doi.org/10.1029/2012JD018323

Feng, M., Biastoch, A., Böning, C., Caputi, N., & Meyers, G. (2008). Seasonal and interannual variations of upper ocean heat balance off the west coast of Australia. *Journal of Geophysical Research*, *113*, C12025. https://doi.org/10.1029/2008JC004908

Feng, M., Hendon, H. H., Xie, S.-P., Marshall, A. G., Schiller, A., Kosaka, Y., et al. (2015). Decadal increase in Ningaloo Niño since the late 1990s. *Geophysical Research Letters*, *42*, 104–112. https://doi.org/10.1002/2014GL062509

Feng, M., Li, Y., & Meyers, G. (2004). Multidecadal variations of Fremantle sea level: Footprint of climate variability in the tropical Pacific. *Geophysical Research Letters*, *31*, L16302. https://doi.org/10.1029/2004GL019947

Feng, M., McPhaden, M. J., Xie, S.-P., & Hafner, J. (2013). La Niña forces unprecedented Leeuwin Current warming in 2011. *Scientific Reports*, *3*(1), 1277. https://doi.org/10.1038/srep01277

Gadgil, S., Joseph, P.-V., & Joshi, N. V. (1984). Ocean-atmosphere coupling over monsoon regions. *Nature*, *312*(5990), 141–143. https://doi.org/10.1038/312141a0

Gill, A. E. (1980). Some simple solutions for heat-induced tropical circulation. *Quarterly Journal of the Royal Meteorological Society*, *106*(449), 447–462. https://doi.org/10.1002/qj.49710644905

Kalnay, E., Kanamitsu, M., Kistler, R., Collins, W., Deaven, D., Gandin, L., et al. (1996). The NCEP/NCAR 40-years reanalysis project. *Bulletin of the American Meteorological Society*, *77*(3), 437–471. https://doi.org/10.1175/1520-0477(1996)077%3C0437:TNYRP%3E2.0.CO;2

Kataoka, T., Tozuka, T., Behera, S., & Yamagata, T. (2014). On the Ningaloo Niño/Niña. *Climate Dynamics*, *43*(5-6), 1463–1482. https://doi.org/10.1007/s00382-013-1961-z

Kataoka, T., Tozuka, T., & Yamagata, T. (2017). Generation and decay mechanisms of Ningaloo Niño/Niña. *Journal of Geophysical Research: Oceans*, *122*, 8913–8932. https://doi.org/10.1002/2017JC012966

Kido, S., Kataoka, T., & Tozuka, T. (2016). Ningaloo Niño simulated in the CMIP5 models. *Climate Dynamics*, *47*(5-6), 1469–1484. https://doi.org/10.1007/s00382-015-2913-6

Kuhnert, H., Pätzold, J., Hatcher, B., Wyrwoll, K.-H., Eisenhauer, A., Collins, L. B., et al. (1999). A 200-year coral stable oxygen isotope record from a high-latitude reef off Western Australia. *Coral Reefs*, *18*(1), 1–12. https://doi.org/10.1007/s003380050147

Liebmann, B., & Smith, C. A. (1996). Description of a complete (interpolated) outgoing longwave radiation dataset. *Bulletin of the American Meteorological Society*, *77*, 1275–1277.

Madden, R. A., & Julian, P. R. (1971). Detections of a 40-50 day oscillation in the tropics. *Journal of the Atmospheric Sciences*, *28*(5), 702–708. https://doi.org/10.1175/1520-0469(1971)028%3C0702:DOADOI%3E2.0.CO;2

Madden, R. A., & Julian, P. R. (1972). Description of global scale circulation cells in the tropics with a 40-50 day period. *Journal of the Atmospheric Sciences*, *29*(6), 1109–1123. https://doi.org/10.1175/1520-0469(1972)029%3C1109:DOGSCC%3E2.0.CO;2

Madec, G. (2008). NEMO ocean engine, Note du Pole de modelisation, Institut Pierre-Simon Laplace (IPSL) No 27, ISSN No 1288-1619.

Marshall, A. G., & Hendon, H. H. (2014). Impacts of the MJO in the Indian Ocean and on the Western Australian coast. *Climate Dynamics*, *42*, 579–595.

Marshall, A. G., Hendon, H. H., Feng, M., & Schiller, A. (2015). Initiation and amplification of the Ningaloo Niño. *Climate Dynamics*, *45*(9-10), 2367–2385. https://doi.org/10.1007/s00382-015-2477-5

Masson, S., Terray, P., Madec, G., Luo, J.-J., Yamagata, T., & Takahashi, K. (2012). Impact of intra-daily SST variability on ENSO characteristics in a coupled model. *Climate Dynamics*, *39*(3-4), 681–707. https://doi.org/10.1007/s00382-011-1247-2

Matsuno, T. (1966). Quasi-geostrophic motions in the equatorial area. *Journal of the Meteorological Society of Japan*, *44*(1), 25–43. https://doi.org/10.2151/jmsj1965.44.1_25

Meyers, G. (1996). Variation of the Indonesian throughflow and the El Niño–Southern Oscillation. *Journal of Geophysical Research*, *101*, 12,255–12,263.

Morioka, Y., Tozuka, T., & Yamagata, T. (2010). Climate variability in the southern Indian Ocean as revealed by self-organizing maps. *Climate Dynamics*, *35*(6), 1059–1072. https://doi.org/10.1007/s00382-010-0843-x

Nordeng, T. E. (1994). Extended versions of the convective parameterization scheme at ECMWF and their impact on the mean sand transient activity of the model in the tropics, ECMWF Research Department, *Tech. Mem.*, *206*, European Centre for Medium Range Weather Forecasts.

Oettli, P., Morioka, Y., & Yamagata, T. (2016). A regional climate mode discovered in the North Atlantic: Dakar Niño/Niña. *Scientific Reports*, *6*(1), 18782. https://doi.org/10.1038/srep18782

Pariwano, J. I., Bye, J. A., & Lennon, G. W. (1986). Long-period variations of sea-level in Australia. *Geophysical Journal of the Royal Astronomical Society*, *87*(1), 43–54. https://doi.org/10.1111/j.1365-246X.1986.tb04545.x

Pearce, A. F., & Feng, M. (2013). The rise and fall of the "marine heat wave" off Western Australia during the summer of 2010/2011. *Journal of Marine Systems*, *111-112*, 139–156. https://doi.org/10.1016/j.jmarsys.2012.10.009

Perkins-Kirkpatrick, S. E., White, C. J., Alexander, L. V., Argüeso, D., Boschat, G., Cowan, T., et al. (2016). Natural hazards in Australia: Heatwaves. *Climate Change*, *139*(1), 101–114. https://doi.org/10.1007/s10584-016-1650-0

Prodhomme, C., Terray, P., Masson, S., Boschat, G., & Izumo, T. (2015). Oceanic factors controlling the Indian summer monsoon onset in a coupled model. *Climate Dynamics*, *44*, 977–1002.

Roeckner, E., Bäuml, G., Bonaventura, L., Brokopf, R., Esch, M., Giorgetta, M., et al. (2003). The atmospheric general circulation model ECHAM 5, Part I, Model description, Report No 349, Max Planck Institute for Meteorology, Hamburg.

Roeckner, E., Brokopf, R., Esch, M., Giorgetta, M., Hagemann, S., Kornblueh, L., et al. (2004). The atmospheric general circulation model ECHAM 5, Part II, Sensitivity of simulated climate to horizontal and vertical resolution, Report No 354, Max Planck Institute for Meteorology, Hamburg.

Saji, N. H., Goswami, B. N., Vinayachandran, P. N., & Yamagata, T. (1999). A dipole mode in the tropical Indian Ocean. *Nature*, *401*(6751), 360–363. https://doi.org/10.1038/43854

Sasaki, W., Doi, T., Richards, K. J., & Masumoto, Y. (2015). The influence of ENSO on the equatorial Atlantic precipitation through the Walker circulation in a CGCM. *Climate Dynamics*, *44*(1-2), 191–202. https://doi.org/10.1007/s00382-014-2133-5

Smith, T. M., Reynolds, R. W., Peterson, T. C., & Lawrimore, J. (2008). Improvements to NOAA's historical merged land-ocean surface temperature analysis (1880–2006). *Journal of Climate*, *21*(10), 2283–2296. https://doi.org/10.1175/2007JCLI2100.1

Terray, P., Kamala, K., Masson, S., Madec, G., Sahai, A. K., & Luo, J.-J. (2012). The role of the intra-daily SST variability in the Indian monsoon variability and monsoon-ENSO-IOD relationships in a global coupled model. *Climate Dynamics*, *39*(3-4), 729–754. https://doi.org/10.1007/s00382-011-1240-9

Tiedtke, M. (1989). A comprehensive mass flux scheme for cumulus parameterization in large-scale models. *Monthly Weather Review*, *117*(8), 1779–1800. https://doi.org/10.1175/1520-0493(1989)117%3C1779:ACMFSF%3E2.0.CO;2

Timmermann, R., Goosse, H., Madec, G., Fichefet, T., Ethe, C., & Duliere, V. (2005). On the representation of high latitude processes in the ORCA-LIM global coupled sea ice-ocean model. *Ocean Modelling*, *8*(1-2), 175–201. https://doi.org/10.1016/j.ocemod.2003.12.009

Tozuka, T., Kataoka, T., & Yamagata, T. (2014). Locally and remotely forced atmospheric circulation anomalies of Ningaloo Niño/Niña. *Climate Dynamics*, *43*(7-8), 2197–2205. https://doi.org/10.1007/s00382-013-2044-x

Turner, N. C., & Asseng, S. (2005). Productivity, sustainability, and rainfall-use efficiency in Australian rainfed Mediterranean agricultural systems. *Australian Journal of Agricultural Research*, *56*(11), 1123–1136. https://doi.org/10.1071/AR05076

Valcke, S. (2006). OASIS3 user guide (prism_2–5). *PRISM support initiative report* 3, pp 64.

Vialard, J., Drushka, K., Bellenger, H., Lengaigne, M., Pous, S., & Duvel, J. P. (2013). Understanding Madden-Julian-induced sea surface temperature variations in the north western Australian Basin. *Climate Dynamics*, *41*(11-12), 3203–3218. https://doi.org/10.1007/s00382-012-1541-7

Wernberg, T., Smale, D. A., Tuya, F., Thomsen, M. S., Langlois, T. J., de Bettignies, T., et al. (2013). An extreme climatic event alters marine ecosystem structure in a global biodiversity hotspot. *Nature Climate Change*, *3*(1), 78–82. https://doi.org/10.1038/nclimate1627

Wijffels, S., & Meyers, G. (2003). An intersection of oceanic waveguides: Variability in the Indonesian Throughflow region. *Journal of Physical Oceanography*, *34*, 1232–1253.

Xie, S.-P., Hu, K., Hafner, J., Tokinaga, H., Du, Y., Huang, G., & Sampe, T. (2009). Indian Ocean capacitor effect on Indo-Western Pacific climate during the summer following El Niño. *Journal of Climate*, *22*(3), 730–747. https://doi.org/10.1175/2008JCLI2544.1

Yuan, C., & Yamagata, T. (2014). California Niño/Niña. *Scientific Reports*, *4*(1), 4801. https://doi.org/10.1038/srep04801

Zhang, N., Feng, M., Hendon, H. H., Hobday, A. J., & Zinke, J. (2017). Opposite polarities of ENSO drive distinct patterns of coral bleaching potentials in the southeast Indian Ocean. *Scientific Reports*, *7*(1), 2443. https://doi.org/10.1038/s41598-017-02688-y

Zinke, J., Rountrey, A., Feng, M., Xie, S.-P., Dissard, D., Rankenburg, K., et al. (2014). Corals record long-term Leeuwin current variability including Ningaloo Niño/Niña since 1795. *Nature Communications*, *5*(1), 3607. https://doi.org/10.1038/ncomms4607